IEEE Access
Multidisciplinary | Rapid Review | Open Access Journal

Received August 22, 2018, accepted September 29, 2018, date of publication October 4, 2018, date of current version October 29, 2018.

Digital Object Identifier 10.1109/ACCESS.2018.2873745

Design and Experimental Research on a Deep-Sea Resonant Linear Ultrasonic Motor

SHAOPENG HE[1], SHENGJUN SHI[1], YUNHE ZHANG[2], AND WEISHAN CHEN[1]
[1]State Key Laboratory of Robotics and System, Harbin Institute of Technology, Harbin 150001, China
[2]Mercedes College, Springfield, SA 5062, Australia

Corresponding author: Shengjun Shi (sirssj@hit.edu.cn)

This work was supported by the National Natural Science Foundation of China under Grant 51575124.

ABSTRACT A deep-sea linear ultrasonic motor, which takes in-plane expansion mode as the working mode, is proposed in this paper. Its main structure is rectangular metal plate with four piezoelectric ceramics. First, suitable structural parameters of the ultrasonic motor are obtained by finite-element simulation. Then, the influences of static seal and the pressures of water on the performance of the ultrasonic motor are studied. Simulation result shows that the static seal slightly degrades the resonant frequency of the ultrasonic motor and vibration amplitude of the driving foot, and the pressures of water almost have no effect on resonant frequency, but it reduces the performance of the ultrasonic motor. Finally, we design and manufacture the prototype, whose velocity is measured at 214 mm/s while the water pressure is 8 MPa and the voltage signal with a frequency of 72 kHz and a voltage magnitude of 200 V. The experimental indicates that simulation results are consistent with experimental results. We verify the feasibility of the ultrasonic motor working in the deep-sea environment.

INDEX TERMS Ultrasonic motors, deep-sea environments, finite element method, asymmetric mode, fluid-solid coupling.

I. INTRODUCTION

Ultrasonic motor is a kind of non-traditional actuator which has the advantages of simple structures, high power with small weight, high precision locating and self -locking by frictional [1]–[7]. It works based on the inverse piezoelectric effect of the piezoelectric ceramics and the frictional coupling of the interface. Ultrasonic motors can work normally by elliptical movements or oblique movements of driving feet and the frictional coupling of the interface [8]–[15]. Those movements are formed by the resonant vibrations of ultrasonic motor, which are generated by the inverse piezoelectric effects of the piezoelectric ceramics [10], [13], [16]–[19]. In the view of the waveform, ultrasonic motors can be classified into two types: standing wave type and travelling wave type. In the view of vibration mode, standing wave type ultrasonic motors can be classified into longitudinal vibrations type, bending vibrations type, in-plane expansion vibration type [16], [20]–[23]. At present, ultrasonic motors have been successfully applied to some industrial applications of medical, automation, spaceflight, etc [24].

There are many minerals, oil, gas resources and plenty of deep-sea biological species to be explored in the deep sea. In the deep sea, the driving actuator needs to withstand the ordeal of the harsh deep-sea environment. Problems such as motive seal, pressure balancing and reliability may exist when traditional motors are used in the deep sea [25], [26]. Motive seal problem is solved by pressure compensation scheme, but this method is unstable [27]. However, ultrasonic motors, which are composed by piezoelectric ceramic and metal structure, can withstand great pressure. In addition, ultrasonic motors can work without coils and magnets, which can greatly simplify the structures [28]–[30]. Thus, we designed an ultrasonic motor that can directly work in the deep-sea environment to solve some problems like motive seal and pressure balancing easily.

In this work, we design a deep-sea resonant linear ultrasonic motor and manufacture the structure corresponding prototype. The structure parameters of the ultrasonic motor are determined by using the finite element analysis. Further the influences of water and static seal on resonant frequency of the ultrasonic motor and amplitude of node on the driving foot are analyzed by the finite element analysis, Next, the experiment platform is constructed to test the performance of prototype. Finally, the experimental data show that experimental

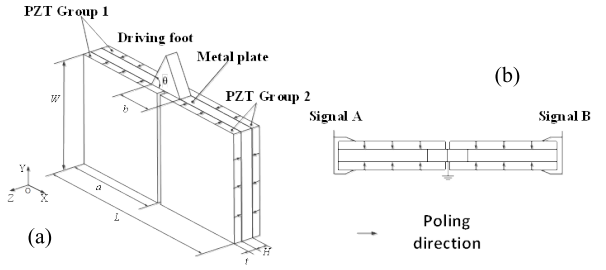

FIGURE 1. Proposed ultrasonic motor: (a) main structure, (b) polarization of PZT.

results are consistent with the simulation results. Thus, it can be recognized that ultrasonic motors can directly work in the deep-sea environment.

II. STRUCTURE AND PRINCIPLE OF THE MOTOR

Ultrasonic motors have satisfying performances in normal environment, but many factors such as added mass of water, pressure of water and static seal make differences in the performances of ultrasonic motors working in deep-sea environment. Ultrasonic motors with different vibration modes and configuration are affected differently by deep-sea environment [31]. An ultrasonic motor with specific configuration which is slightly affected by the deep-sea environment is studied in this work. This configuration, which is presented by Oleksiy Vyshnevskyy, has a simple structure. This configuration make use of a single in-plane expansion vibration called asymmetrical E (3,1) vibration [23]. The single in-plane expansion vibration mode has two advantages: It doesn't have to adjust parameters to complete vibration frequency degeneration; it gets small influence by deep-sea environments.

The stator of the ultrasonic motor is symmetrical about the xoy and yoz as show in Fig.1 (a). It is composed of the aluminum plate whose length is twice as long as its width and four rectangular piezoelectric ceramics. The thick of aluminum plate is 3 mm, and the thick of the piezoelectric ceramics is 1 mm. The driving foot, which is a triangle plate metal, is placed in the middle of longer side. Four piezoelectric ceramics whose polarization directions in each group are opposite are divided into two groups. As show in Fig.1 (b), A phase voltage is applied to one group of the ceramics, and B phase voltage is applied to the other group. The asymmetric E (3,1) vibration mode is excited by switching on A phase voltage and switching off B phase voltage. The motion of opposite direction can be got by switching off A phase voltage and switching on B phase voltage.

Ultrasonic motors generate movements by elliptical movements or oblique movements of the driving feet and the frictional coupling of the interface. The ultrasonic motor studied in this work adopts the in-plane expansion vibration mode which is the asymmetrical E (3,1) vibration mode of the rectangular plate to generate oblique movements of the driving foot, as shown in Fig.2.

Fig.3 shows that the motion of the driving foot of ultrasonic motor is divided into four stages: When t = 0, the stator is

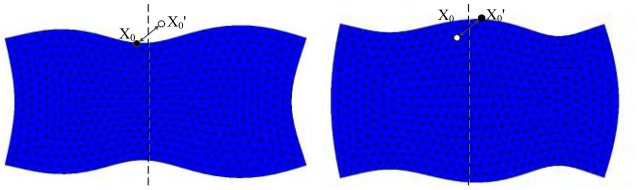

FIGURE 2. Asymmetrical E(3,1) modal vibration mode.

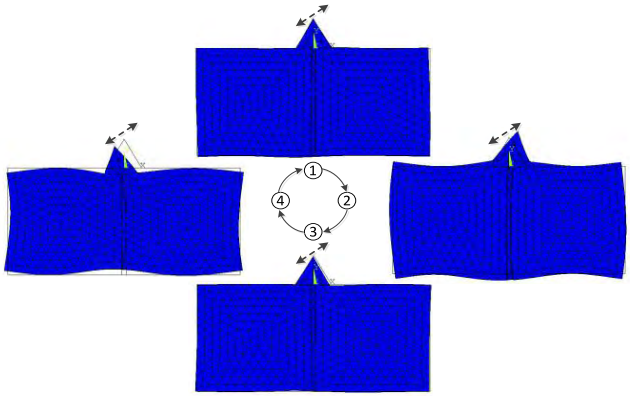

FIGURE 3. Vibration modal of the ultrasonic motor in a cycle .

in ① state and the driving foot is at the equilibrium position; When t = T /4, the stator is in ② state and generates the expansion deformation. The driving foot is in position of the biggest expansion deformation; When t = T/2, the stator is in ③ state and the driving foot returns to the equilibrium position. When t = 3T/4, the stator is in ④ state and generates the contraction deformation. The driving foot is in position of the biggest contraction deformation; When t = T, the stator returns to state ①. It can be observed that the oblique movement to contribute to the movement of ultrasonic motor is got.

III. MOTOR ANALYSIS BY FEM

The motor analyses mainly include the modal analysis and the transient analysis. In the modal analysis, the specific vibration mode and the resonant frequency need to be found. In the transient analysis, the movement of the node of the driving foot can be obtained to judge the feasibility of the ultrasonic motor. Firstly, the basic parameters of the stator are preliminarily determined as shown in the table 1. Next, the base line of the triangular driving foot (b) and the angle of the triangle (θ) are determined by the finite element analysis. Then, the influence of static seal and water on the ultrasonic motor are studied. Finally, the simulation result of the ultrasonic motor is got to manufacture prototype.

A. DETERMINING THE STRUCTURE PARAMETERS

The simple variable method is used to determine the parameters of driving foot. Finite element models are built according to different driving foot lengths which are adjusted from 4 mm to 12 mm. The driving foot angle of the finite element models is 60°. The maximum amplitude of node on the

TABLE 1. Basic structure parameters.

rectangular plate			piezoelectric ceramic	
length L (mm)	width W (mm)	thickness H (mm)	length a (mm)	Thickness t (mm)
53	26	3	26	1

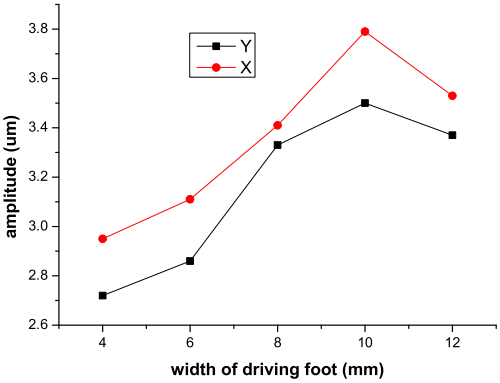

FIGURE 4. Relationship between width of driving foot and displacement of the driving foot.

driving foot in different directions with different driving foot width is got by the finite element analysis as shown in Fig.4. It should be note that the amplitudes of the X direction and the Y direction increase with the driving foot length increasing from 4mm to 10mm, however the amplitudes of the X direction and the Y direction decreases when the driving foot length exceed 10mm. Therefore, the driving foot length is set as 10mm to get better movement.

When driving foot length is determined, the finite element models are built according to different angles which are adjusted from 40° to 60°. The driving foot length of the finite element models is 10mm. The relationship between driving foot angle and maximum amplitude of node on the driving foot is got as shown in Fig.5. It should be note that the X-axis amplitude of the driving foot increases, however the Y-axis amplitude of the driving foot decreases with increasing of the driving foot angle from 40° to 60°. Therefore, the angle of the driving foot is set as 52° to have best characteristics. Finally, all parameters are determined as shown in table2.

B. MODAL AND TRANSIENT ANALYSIS BEFORE INSULATED ENCAPSULATION

When all structure parameters are determined, we carry out finite element analysis of ultrasonic motor modal without water. In the modal analysis, we find the E (3,1) vibration mode of the modal and its resonant frequency, which is 81.62 kHz. In the transient analysis, the phase voltage with frequency of 81.62 kHz and voltage of 100 V is applied to one group ceramics. As shown in Fig.6, it should be note that the amplitude of node on the driving foot reaches the state of stable vibrations after a certain amount of time. it can be observed that the x-axis amplitude and the y-axis

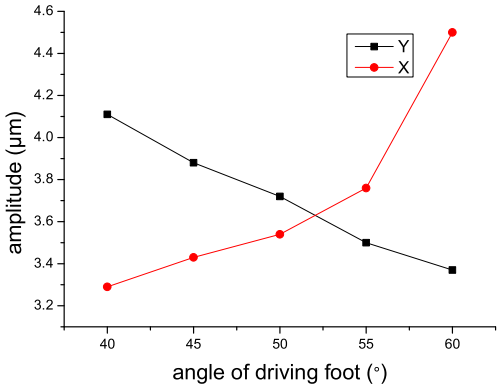

FIGURE 5. Relationship between angle of driving foot and displacement of the driving foot.

TABLE 2. All structure parameters.

rectangular plate			piezoelectric ceramic		driving foot	
length L (mm)	width W (mm)	thickness H (mm)	length a (mm)	Thickness t (mm)	length b (mm)	Angle θ (°)
53	26	3	26	1	10	52

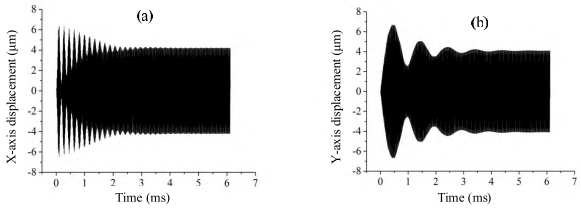

FIGURE 6. Displacements of driving foot: (a) along x, (b) along y.

amplitude is 4.05 μm and 4.1 μm respectively as shown in Fig.6. The movement of the driving foot is oblique ellipse trajectory which is similar to oblique as shown in Fig.7, which contributes to the movement of ultrasonic motor. The oblique ellipse trajectory is generated by the different damping of simulation. It can be recognized that this ultrasonic motor can theoretically work in normal environment.

C. MODAL AND TRANSIENT ANALYSIS AFTER INSULATED ENCAPSULATION

This ultrasonic motor, which works in deep-sea environment, requires the static seal to ensure the insulation. Thanks to the characteristics of good resilience and the high mechanical strength, the silicone rubber is chosen as packaging material. The encapsulation modal whose insulation layer thickness is 1mm is built, as shown in Fig.8. After the static seal, the model and transient analysis should to be carried out again. The resonant frequency of this model is got by the modal analysis, which reduces to 80.69 kHz. In the transient analysis, the corresponding voltage signal with frequency of 80.69 kHz and voltage of 100V is applied to the ceramics.

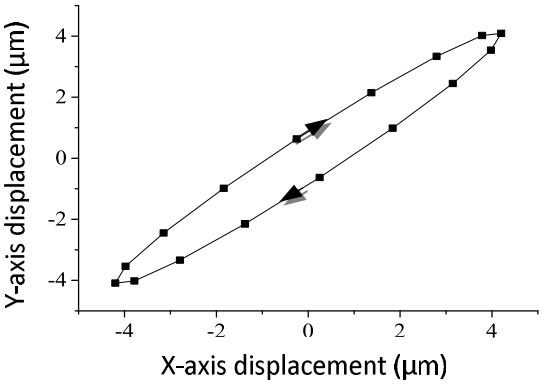

FIGURE 7. Motion trail of the driving foot.

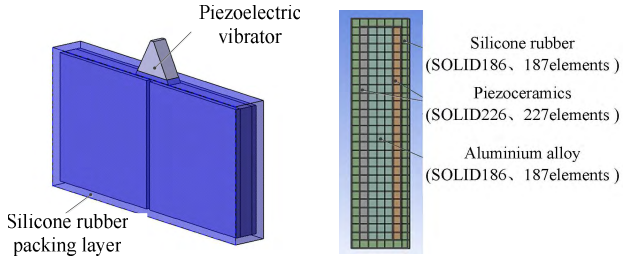

FIGURE 8. Encapsulation model of ultrasonic motor.

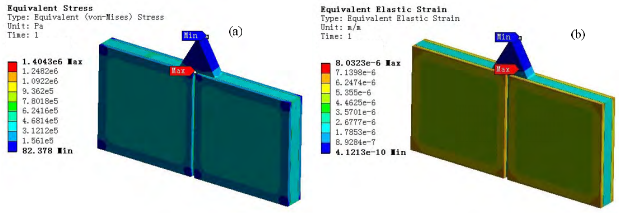

FIGURE 9. The cloud diagram at 20 MPa: (a) equivalent stress, (b) equivalent strain.

The simulation result shows the amplitude of X-axis and Y-axis reduces to 3.90 μm and 3.9 μm respectively. It can be observed that the static seal has small influence on result of simulation.

D. WET MODAL AND TRANSIENT ANALYSIS AFTER INSULATED ENCAPSULATION

To get the influences of the pressure on the ultrasonic motor, the pre-loaded pressure analysis before the wet modal analysis is carried out. Different pressures from 0 to 20 MPa are added to the surface of model, but we get almost the same resonant frequency with different pressures. When the pressure is 20 MPa, the resonant frequency, which is 82.34 kHz, is slightly higher than the result without pressure. It can be recognized that pressure of water almost has little effect on the resonant frequency. It can be observed that the maximum stress and strain can't break the structure of ultrasonic motor as shown in Fig.9.

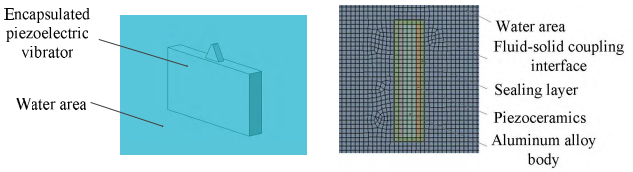

FIGURE 10. Model of the ultrasonic motor under the water.

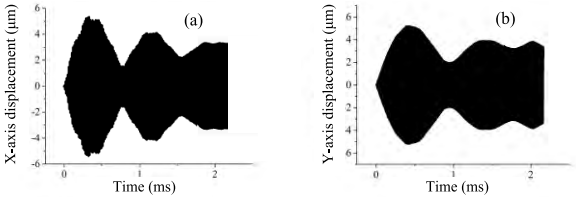

FIGURE 11. Displacements of driving foot: (a) along x, (b) along y.

After the pre-loaded pressure analysis, the wet modal analysis is conducted. ANSYS does not have the infinite area to simulate sea area, However many researches indicate that the analysis result is exact when water is five times the volume of ultrasonic motor. The simulation model whose volume of water is five-fold volume of ultrasonic motor is built, as shown in Fig.10. The acoustic element Fluid 220 and Fluid 221 elements are used to imitate water by defining density and sound velocity. The contact surface of actuator and water are defined as fluid solid interface. The nodes on the fluid solid interface have four degrees of freedom: the Pressure, Ux, Uy and Uz. After the modal is built, the asymmetrical method was used to conduct the wet modal analysis of the ultrasonic motor. We also find the E (3,1) vibration mode of the modal and its resonant frequency, which is 74.35 kHz, reduced by 8.93% compared with that of the normal environment.

Transient analysis was accomplished to investigate the vibration trajectories of the driving foot. In the transient analysis, the voltage signal with frequency of 74.35 kHz and voltage of 100 V is applied to one group ceramics. The amplitudes of node on driving foot are got as shown in Fig.11. It should be note that the amplitude in X direction of the driving foot is 3.08 μm , which reduced by 24.90% compared with that of the normal environment. The Y-axis maximum amplitude of the driving foot is 3.56 μm, which reduced by 12.02% compared with that of the normal environment. The movement of the node on driving foot is an oblique ellipse trajectory which is similar to oblique as shown in Fig.12. The oblique ellipse trajectory is generated by the different damping of simulation. It can be observed that the ultrasonic motor can theoretically work in the deep-sea environments.

IV. EXPERIMENTS AND MOTOR CHARACTERISTICS

To validate the simulation result, we manufacture the prototype, experimental platform and the deep sea high pressure simulation system. We manufacture the prototype is manufactured by piezoelectric ceramics and the structural body. Four bolts are used to fix the stator of the ultrasonic motor,

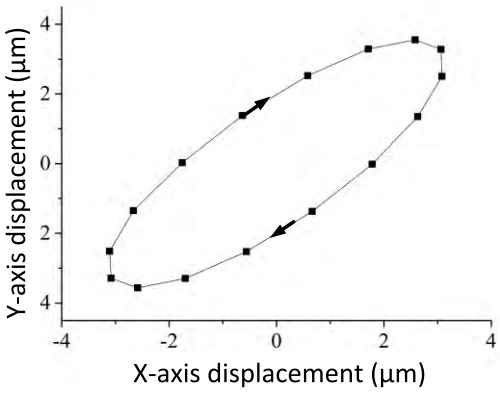

FIGURE 12. Vibration track of the driving foot of the ultrasonic motor.

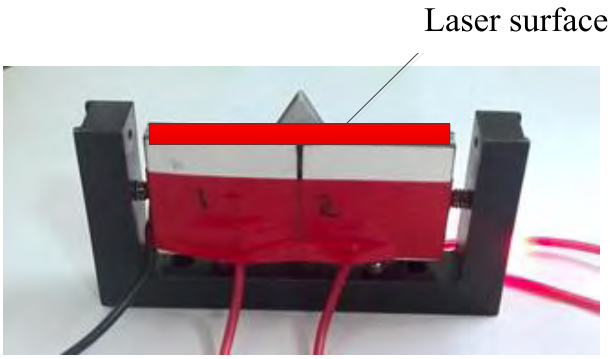

FIGURE 13. The prototype of ultrasonic motor.

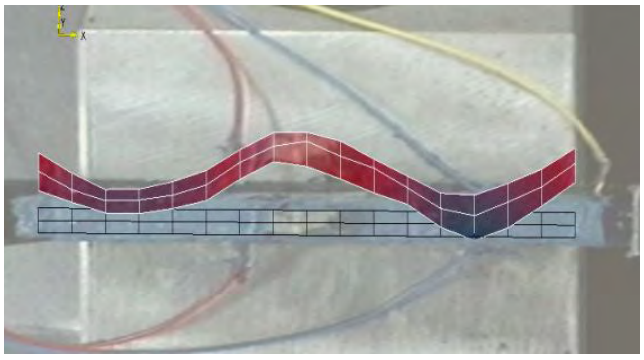

FIGURE 14. The vibration shape of prototype.

as shown in the Fig.13. Next, the scanning laser Doppler vibrometer (PSV-400-M2, Polytec, Germany) is used to measure prototype's vibration mode and the resonant frequency, as shown in Fig.14 and Fig.15. The test surface is selected as shown in Fig.13. It should be note that the vibration mode is almost coincident with the simulation result. The resonant frequency was 82.63 kHz, which increased by 0.35% compared with that of simulation result, which can be explained as that the fabrication error contribute on the little difference.

The prototype is placed in the experimental platform, as shown in Fig.16. Both sides of the prototype are slidable, so that we can control the pre-tightening up force by adjusting

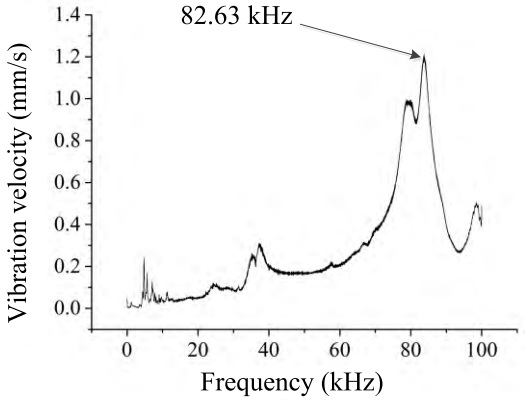

FIGURE 15. The vibration velocity response spectrum.

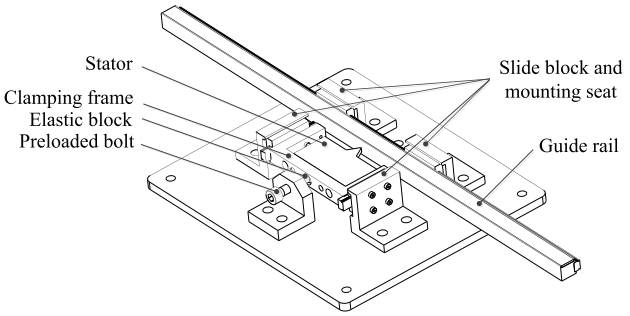

FIGURE 16. The experimental facility of prototype.

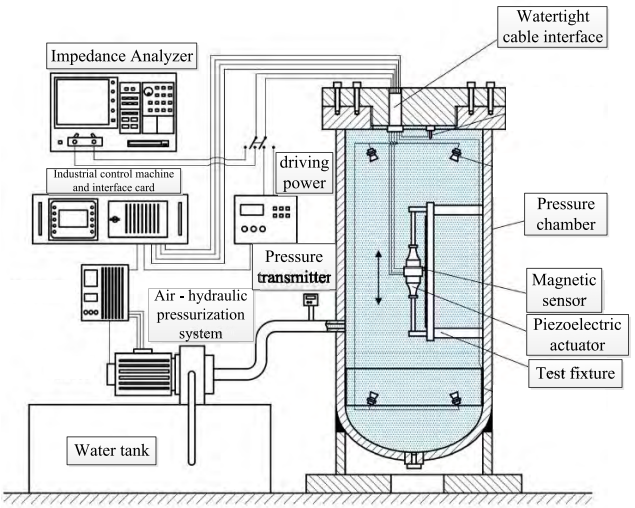

FIGURE 17. The deep sea high pressure simulation system.

the preloaded bolt. When prototype works, the guide rail will run by the frictional force of interface. The velocity of the guide rail is tested to reveal the performance of prototype.

As shown in Fig.17, the deep sea high pressure simulation system is designed to simulate experimental environment. The Air - hydraulic pressurization system provides a pressure up to 50MPa for the experimental system. Watertight cable can provide the sealed environment and contact measuring

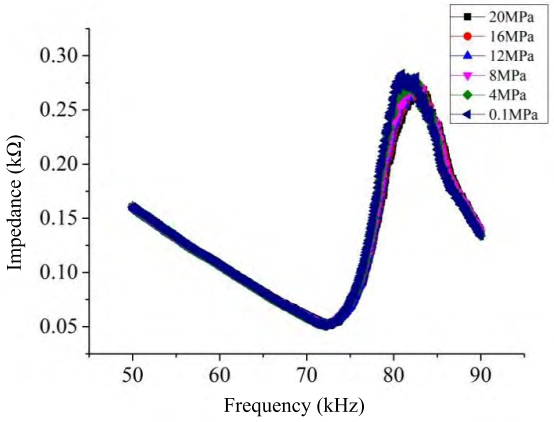

FIGURE 18. Impedance curve of the stator in pressured water.

TABLE 3. Underwater motion characteristics test data.

Voltage V	pressure MPa	Frequency kHz	Velocity mm/s	Accelerated velocity m/s^2
200	0.1	72	342	6.37
200	2	72	340	6.32
200	4	72	280	5.16
200	6	72	223	4.00
200	8	72	114	2.14

instrument and hyperbaric cabin. Magnetic sensor can measure the velocity of guide rail in the low pressure.

After previous measurement, the sealed prototype is placed in the deep sea high pressure simulation system. The measure impedance characteristic of prototype with different water pressure from 0.1 MPa to 20 MPa are measured by the precision impedance analyzer. The impedance curves have high consistency while the water pressure varied from 0.1 MPa to 20 MPa as shown in Fig.18. It can be recognized that the pressure has little effect on the resonant frequency of ultrasonic motor, which accord with the simulation result well. Thus, ultrasonic motor can be excited with voltage signal of the same frequency and different depth of water.

In the high pressure simulation system, only the velocity of guide rail can be measured, which weight 310 g. The start and close test is conducted to measure velocity and acceleration. The simulation results of underwater and apparatus testing result of prototype show the resonant frequency is similar to 74 kHz. But the actual testing result shows the performance is bested with the frequency of 72 kHz. During the testing, the voltage signal with frequency of 72 kHz and voltage of 200 V was applied on the ultrasonic motor. The prototype can complete the reciprocating movement by adjusting the signaling switch. The velocity and accelerated velocity of guide rail with the different intensity of pressure are shown in table 3. The Velocity-time curve and acceleration-time curve with different intensity of pressure are shown in Fig.19. It should be note that the motion curve is regular,

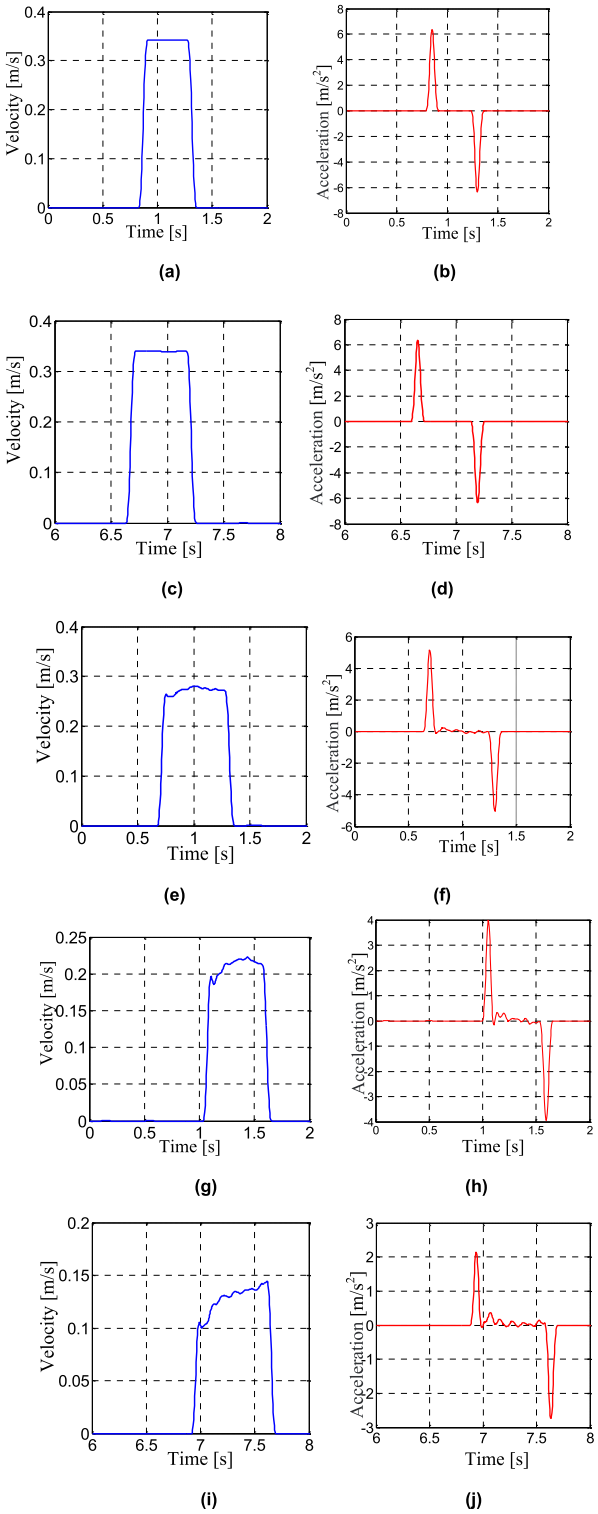

FIGURE 19. Velocity-time curve and acceleration-time curve with different intensity of pressures: (a) velocity-time curve with 0.1 MPa, (b) acceleration-time curve with 0.1 MPa, (c) velocity-time curve with 2 MPa, (d) acceleration-time curve with 2 MPa, (e) velocity-time curve with 4 MPa, (f) acceleration-time curve with 4 MPa, (g) velocity-time curve with 6 MPa, (h) acceleration-time curve with 6 MPa, (i) velocity-time curve with 8 MPa, (j) acceleration-time curve with 8 MPa.

which verify that ultrasonic motor working in the deep-sea environment still has a good character of start and close. However velocity and acceleration of the prototype decrease with the increase of pressure. There are two reasons for this decrease. On the one hand, the contact condition of stator and rotor changes with the pressure increase, so that the pre-compression changes. On the other hand, loss of vibration increases with the pressure increase, so that amplitude of driving foot has a decrease.

V. CONCLUSION

In this work, we propose a deep-sea resonant linear ultrasonic motor and make up prototype to verify the simulation result. Experimental results show that the static seal and pressure have little influence on the resonant frequency. However, pressure of the water reduces the performance of ultrasonic motor, factors leading to that are proposed in this paper. It can be observed from the experiment that the velocity of ultrasonic motor is 214 mm/s while the water pressure is 8 MPa and the voltage signal with frequency of 72 kHz and voltage of 200 V. The ultrasonic motor can properly work in the deep-sea environment. It can be verified that deep-sea ultrasonic motor has bright prospects in terms of deep-sea exploitation.

REFERENCES

[1] H. J. M. T. S. Adriaens, W. L. De Koning, and R. Banning, "Modeling piezoelectric actuators," *IEEE/ASME Trans. Mechatronics*, vol. 5, no. 4, pp. 331–341, Dec. 2000.

[2] K. Asumi, R. Fukunaga, T. Fujimura, and K. K. Minoru, "High speed, high resolution ultrasonic linear motor using V-shape two bolt-clamped Langevin-type transducers," *J. Acoust. Soc. Jpn.*, vol. 30, no. 3, pp. 180–186, 2009.

[3] E. Golubovic, Z. Zhakypov, T. Uzunovic, and A. Sabanovic, "Piezoelectric motor driver: Design and evaluation," in *Proc. 39th Annu. Conf. IEEE Ind. Electron. Soc.*, Nov. 2013, vol. 20, no. 11, pp. 203–208.

[4] Y. Liu, W. Chen, J. Liu, and S. Shi, "A cylindrical traveling wave ultrasonic motor using longitudinal and bending composite transducer," *Sens. Actuators A, Phys.*, vol. 161, nos. 1–2, pp. 158–163, 2009.

[5] Y. Liu, W. Chen, J. Liu, and S. Shi, "A cylindrical standing wave ultrasonic motor using bending vibration transducer," *Ultrasonics*, vol. 51, no. 5, pp. 527–531, 2011.

[6] Y. Liu, W. Chen, D. Shi, X. Tian, S. Shi, and D. Xu, "Development of a four-feet driving type linear piezoelectric actuator using bolt-clamped transducers," *IEEE Access*, vol. 5, pp. 27162–27171, 2017.

[7] Y. Liu, W. Chen, X. Yang, and J. Liu, "A rotary piezoelectric actuator using the third and fourth bending vibration modes," *IEEE Trans. Ind. Electron.*, vol. 61, no. 8, pp. 4366–4373, Aug. 2014.

[8] P. Hagedorn and J. Wallaschek, "Travelling wave ultrasonic motors—Part I: Working principle and mathematical modelling of the stator," *J. Sound Vibrat.*, vol. 155, no. 1, pp. 31–46, 1992.

[9] B. Koc and K. Uchino, "Piezoelectric ultrasonic motors," Tech. Rep., 2000.

[10] J. Liu, Y. Liu, L. Zhao, D. Xu, W. Chen, and J. Deng, "Design and experiments of a single-foot linear piezoelectric actuator operated in a stepping mode," *IEEE Trans. Ind. Electron.*, vol. 65, no. 10, pp. 8063–8071, Oct. 2018.

[11] Y. Liu, W. Chen, J. Liu, and X. Yang, "A high-power linear ultrasonic motor using bending vibration transducer," *IEEE Trans. Ind. Electron.*, vol. 60, no. 11, pp. 5160–5166, Nov. 2013.

[12] Y. Liu, W. Chen, X. Yang, and J. Liu, "A T-shape linear piezoelectric motor with single foot," *Ultrasonics*, vol. 56, pp. 551–556, Feb. 2015.

[13] Y. Liu, L. Wang, Z. Gu, Q. Quan, and J. Deng, "Development of a two-dimensional linear piezoelectric stepping platform using longitudinal-bending hybrid actuators," *IEEE Trans. Ind. Electron.*, to be published.

[14] Z. Zhakypov, E. Golubovic, T. Uzunovic, and A. Sabanovic, "High precision control of a walking piezoelectric motor in bending mode," in *Proc. 9th Asian Control Conf. (ASCC)*, Jun. 2013, pp. 1–6.

[15] Q. Zhang, W. Chen, Y. Liu, J. Liu, and Q. Jiang, "A frog-shaped linear piezoelectric actuator using first-order longitudinal vibration mode," *IEEE Trans. Ind. Electron.*, vol. 64, no. 3, pp. 2188–2195, Mar. 2017.

[16] X. Yang, Y. Liu, W. Chen, and X. Zhao, "New excitation method for sandwich transducer using bending composite vibrations: Modeling, simulation, and experimental evaluation," *IEEE Trans. Ind. Electron.*, vol. 65, no. 6, pp. 4889–4896, Jun. 2018.

[17] K. Yokoyama, H. Tamura, K. Masuda, and T. Takano, "Single-phase drive ultrasonic linear motor using a linked twin square plate vibrator," *Jpn. J. Appl. Phys.*, vol. 52, no. 7S, pp. 07HE03-1–07HE03-7, Jun. 2013.

[18] S. Yuan, Y. Zhao, X. Chu, C. Zhu, and Z. Zhong, "Analysis and experimental research of a multilayer linear piezoelectric actuator," *Appl. Sci.*, vol. 6, no. 8, p. 225, 2016.

[19] C.-H. Yun, T. Ishii, K. Nakamura, S. Ueha, and K. Akashi, "A high power ultrasonic linear motor using a longitudinal and bending hybrid bolt-clamped Langevin type transducer," *Jpn. J. Appl. Phys.*, vol. 40, no. 5B, pp. 3773–3776, 2001.

[20] Y. Liu, J. Yan, D. Xu, W. Chen, X. Yang, and X. Tian, "An I-shape linear piezoelectric actuator using resonant type longitudinal vibration transducers" *Mechatronics*, vol. 40, pp. 87–95, Dec. 2016.

[21] P. Smithmaitrie, P. Suybangdum, P. Laoratanakul, and N. Muensit, "Design and performance testing of an ultrasonic linear motor with dual piezoelectric actuators," *IEEE Trans. Ultrason. Ferroelectr. Freq. Control*, vol. 59, no. 5, pp. 1033–1042, May 2012.

[22] J.-J. Tzen, S.-L. Jeng, and W.-H. Chieng, "Modeling of piezoelectric actuator for compensation and controller design," *Precis. Eng.*, vol. 27, no. 1, pp. 70–86, 2003.

[23] O. Vyshnevskyy, S. Kovalev, and W. Wischnewskiy, "A novel, single-mode piezoceramic plate actuator for ultrasonic linear motors," *IEEE Trans. Ultrason. Ferroelectr. Freq. Control*, vol. 52, no. 11, pp. 2047–2053, Nov. 2005.

[24] Y. Shi, Y. Li, C. Zhao, and J. Zhang, "A new type butterfly-shaped transducer linear ultrasonic motor," *J. Intell. Mater. Syst. Struct.*, vol. 22, no. 6, pp. 567–575, 2011.

[25] Y. Xu, Y. Wei, J. Zou, J. Li, W. Qi, and Y. Li, "Estimation of the iron loss in deep-sea permanent magnet motors considering seawater compressive stress," *Sci. World J.*, vol. 2014, no. 2, 2014, Art. no. 265816.

[26] J. Zou, W. Qi, Y. Xu, F. Xu, Y. Li, and J. Li, "Design of deep sea oil-filled brushless DC motors considering the high pressure effect," *IEEE Trans. Magn.*, vol. 48, no. 11, pp. 4220–4223, Nov. 2012.

[27] N. Vedachalam *et al.*, "Challenges in realizing robust systems for deep water submersible ROSUB6000," in *Proc. IEEE Int. Underwater Technol. Symp. (UT)*, Mar. 2013, pp. 1–10.

[28] Y. Liu, X. Yang, W. Chen, and D. Xu, "A bonded-type piezoelectric actuator using the first and second bending vibration modes," *IEEE Trans. Ind. Electron.*, vol. 63, no. 3, pp. 1676–1683, Mar. 2016.

[29] P. S. Schenker *et al.*, "Composite manipulator utilizing rotary piezoelectric motors: New robotic technologies for Mars *in-situ* planetary science," vol. 3041, pp. 918–926, Jun. 1997.

[30] S. Shao, M. Xu, S. Zhang, and S. Xie, "Stroke maximizing and high efficient hysteresis hybrid modeling for a rhombic piezoelectric actuator," *Mech. Syst. Signal Process.*, vol. 75, pp. 631–647, Jun. 2016.

[31] J. Gao *et al.*, "The effect of the hydrostatic pressure on the electromechanical properties of ferroelectric rhombohedral single crystals $Pb(Mg_{1/3}Nb_{2/3})$-$Pb(In_{1/2}Nb_{1/2})$-$PbTiO_3$," *Appl. Phys. Lett.*, vol. 99, no. 6, p. 1804, 2011.

SHAOPENG HE was born in Hebei, China, in 1994. He received the B.S. degree in mechanical engineering from the Harbin Institute of Technology, China, in 2016, where he is currently pursuing the Ph.D. degree. His research interest is ultrasonic motor.

SHENGJUN SHI was born in Heilongjiang, China, in 1974. He received the B.S. degree in aircraft manufacturing engineering from Northwest Polytechnical University in 1997 and the M.S. and Ph.D. degrees from the School of Mechatronics Engineering, Harbin Institute of Technology, China, in 2003 and 2007, respectively. He is currently an Associate Professor with the Harbin Institute of Technology. His research interests include ultrasonic motor and ultrasonic application.

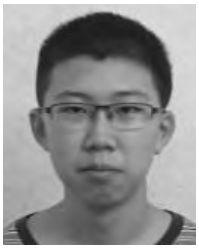

YUNHE ZHANG was born in Heilongjiang, China, in 1999. He attended high school in the Mercedes College, Adelaide, Australia, where he is currently enrolled in the IB Diploma Program and will be graduated this year. He is a focused and patient person who is skilled in mathematics and science. Since he was in the middle school, he developed his passion in physics and chemistry.

WEISHAN CHEN was born in Hebei, China, in 1965. He received the B.S. and M.S. degrees in precision instrumentation engineering and the Ph.D. degree in mechatronics engineering from the Harbin Institute of Technology, Harbin, China, in 1986, 1989, and 1997, respectively. Since 1999, he has been a Professor with the School of Mechatronics Engineering, Harbin Institute of Technology. His research interests include ultrasonic driving, smart materials and structures, and bio-robotics.